Available online at www.sciencedirect.com

ScienceDirect

Procedia Manufacturing 15 (2018) 1864–1871

Procedia MANUFACTURING

www.elsevier.com/locate/procedia

17th International Conference on Metal Forming, Metal Forming 2018, 16-19 September 2018, Toyohashi, Japan

Computer simulations of austenite decomposition of hot formed steels during cooling

Aarne Pohjonen*, Antti Kaijalainen, Juho Mourujärvi, Jari Larkiola

Department of Materials and Production Technology, University of Oulu, 90014, Oulu, Finland

Abstract

Hot deformation and cooling together with the chemical composition define the final mechanical properties of the steel product. In order to control and optimize the desired properties, quantitative models are needed. In this article we present our phase transformation model, which has been fitted to experimental continuous cooling data and coupled to our own heat conduction computer simulation software. The fitting of the model to experimental data enables accurate modeling. The coupled heat transfer and conduction models allow the simulation of non-uniform cooling rates and temperature distribution. The development of our own software enables full control and easy linking of the models in order to use them in modeling and optimizing cooling procedures. The presented phase transformation model also provides information on the onset and kinetics, which can be used in more detailed microstructure models. The transformation model can also be introduced in other simulation softwares as a subroutine.

Peer-review under responsibility of the scientific committee of the 17th International Conference on Metal Forming.

Keywords: Steel; Water cooling; Phase transformations; Bainite; Martensite; Ferrite

* Corresponding author. Tel.: +358-505974261; Fax: +358-8-344-084
E-mail address: Aarne.Pohjonen@Oulu.fi

2351-9789
Peer-review under responsibility of the scientific committee of the 17th International Conference on Metal Forming.
10.1016/j.promfg.2018.07.203

Nomenclature

T	Temperature
τ	Time required for transformation to start during isothermal holding
$\dot{\theta}$	Cooling rate
K	Fitting parameter for incubation time calculation
A	Fitting parameter for incubation time calculation
m	Fitting parameter for incubation time calculation
Q	Fitting parameter for incubation time calculation (Activation energy)
R	Ideal gas constant, 8.314 J/(K mol)
Δt	Time step
$\chi_{\max}$	Maximum phase fraction
k	Temperature dependent rate parameter
n	Fitting parameter for kinetic model (Avrami exponent)
a	Fitting parameter for kinetic model
b	Fitting parameter for kinetic model
c	Fitting parameter for kinetic model
C_0	Initial austenite carbon content (wt %)
C_γ	Austenite carbon content (wt %)
η	Fitting parameter for martensite transformation
M_s	Fitting parameter for martensite transformation (Martensite start temperature)
ρ	Density
c	Specific heat capacity
κ	Heat conductivity
s	Source term in heat equation, energy increase per volume
$\dot{q}$	Heat flux
h_{eff}	Effective heat transfer coefficient
T_{ext}	External temperature
$\hat{n}$	Unit surface normal vector
W	Water flux in l/(m^2 s)
x_i	Spatial coordinates

1. Introduction

The growing demand for energy efficient solutions has increased the use of ultra high strength steels (UHSS) constantly. High strength with sufficient formability allows light weight design for numerous steel applications. Thinner wall thicknesses of high yield strength steels can allow clear weight-savings compared to conventional steels. Direct quenching of low-carbon thermomechanically rolled steel is a cost-efficient processing route to produce ultra high strength steels. There is no need for additional tempering heat treatment to achieve required mechanical properties. The microstructures of these steels often comprise lower bainite and/or auto-tempered martensite. During the development of these steels, the main focus is concerned with understanding the inter-relationships between processing and fabrication parameters on the evolution of microstructure and thus the mechanical properties. However, besides a good knowledge of metallurgy, the development of such steels requires a lot of experimental tests.

The object of our work is to go towards digitalized steel development which means less experimental work utilizing accurate simulation tools. This provides significant cost and time savings by speeding up the development work of the new steel product and shortening the time to market. The computing of austenite decomposition is an important part of this simulation environment. A transformation model has been used as a subroutine in FE-analyses and input for cellular automata simulations to predict phase fractions and microstructure after hot rolling and accelerated cooling.

2. Theory

In order to calculate the phase transformations occurring during water cooling of hot rolled steel, we use our own phase transformation code, which has been fully coupled to our own heat conduction simulation codes. The phase transformation model has also been written as a subroutine to a commercial finite element code Abaqus [1]. The model includes calculation for the transformation start and the kinetics after the onset. The latent heat released due to the transformation is taken in to account in the heat conduction simulations. The heat conductivity, density and heat capacity depend on the transformed fraction as well as temperature. All codes were implemented by the first author of this article.

2.1. Phase transformations

To take in to account for the incubation phenomena we calculated the transformation start using the concept of ideal TTT diagram [2, 3], as described in [4] for the same steel as studied in this article. Shortly, using the linear continuous cooling data we calculated the time τ which would be required for the transformation to start during isothermal holding at temperature T by $\tau(T) = -(d\dot{\theta}(T)/dT)^{-1}$, where $\dot{\theta}(T)$ is the cooling rate required for the transformation to start at temperature T during cooling with linear cooling path. The functional form $\tau(T) = K(A-T)^{-m}\exp[Q/(R(T+273.15)]$ with fitting parameters K, A, m and Q was used. An estimate for the transformation start (assumed as 1% transformed) for arbitrary thermal path is then calculated with the rule of Scheil, i.e. the transformation is assumed to start once the sum $\sum \Delta t/\tau(T)$ equals unity, where Δt is the time spent at temperature T. Once the transformation start has been reached, the kinetics are calculated with the following differential form of Johnson-Mehl-Avrami-Kolmogorov equation [5, 6]:

$$\frac{d\chi}{dt} = (\chi_{\max} - \chi)\left[\ln\left(\frac{\chi_{\max}}{\chi_{\max} - \chi}\right)\right]^{\frac{n-1}{n}} nk^{1/n}, \tag{1}$$

where k is the temperature dependent rate parameter, and n is a fitting parameter which was assumed as constant. For ferrite the temperature dependent maximum phase amount $\chi_{f,\max}$ is calculated using lever rule from the equilibrium diagram, as described in ref. [6, 7, 8] for the untransformed austenite. For bainite and martensite the maximum phase fraction is the fraction of untransformed austenite $\chi_{b,\max} = 1 - \chi_f - \chi_m$ and $\chi_{m,\max} = 1 - \chi_f - \chi_b$ where the subscripts *f*, *b,* and *m* are used to denote the fractions of ferrite, bainite and martensite. The temperature dependence of the parameter k was described with Eq. (2)

$$\begin{aligned} k_f &= \exp(-a_f(T-b_f)^2 - c_f) \qquad \text{for ferrite,} \\ k_b &= \frac{C_0}{C_\gamma}\exp(-a_b(T-b_b)^2 - c_b) \qquad \text{for bainite,} \end{aligned} \tag{2}$$

where a, b and and c are fitting constants. To take in to account the austenite carbon enrichment the fraction C_0/C_γ was used in the front of bainite parameter k_b. The equilibrium austenite carbon content C_γ was calculated as $C_\gamma = (C_0 - \chi_f C_f)/(1-\chi_f)$, where C_0 is the initial austenite carbon content and C_f is the ferrite carbon content. The martensite transformation was modeled applying the Koistinen-Marburger type equation, i.e. $\chi_{m,\max} = 1 - \exp[-\eta(M_s - T)]$, where the parameter η and the martensite start temperature M_s were fitted to experimental data [9].

2.2. Heat conduction and transfer

In order to simulate the heat conduction inside of the steel strip, we solve the heat equation (3)

$$\rho c \frac{\partial}{\partial t} T = \nabla \bullet \left(\kappa \nabla T \right) + s, \tag{3}$$

where the density ρ, specific heat c and heat conductivity κ depend on both temperature and transformed austenite fraction, as described in [6, 8, 10, 11]. The latent heat released due to transformation occurring during simulation time step is included in the source term s. To calculate the heat flux $\dot{q}$ due to spray water cooling, we apply the effective temperature dependent heat transfer coefficient $h_{eff} = \dot{q} / (T - T_{ext})$. Since the heat flux is related to the temperature gradient by Fourier's law the temperature gradient at the surface can be defined by Eq. (4)

$$\nabla T = \frac{h_{eff}}{\kappa} (T - T_{ext}) \hat{n} \, . \tag{4}$$

To simulate spray water cooling of a steel strip, we applied the Eq. (5) [8, 12], which describes the dependence of h_{eff} on water flux and the strip surface temperature.

$$\begin{aligned} h_{eff} &= 3.16 \times 10^9 \zeta_1 \left[(T - T_1) - \zeta_2 (T - T_3) \right]^{-2.455} W^{0.616}, \\ \zeta_1 &= 1 - 1 / (1 + \exp[(T - T_2) / 40]), \\ \zeta_2 &= 1 - 1 / (1 + \exp[(T - T_3) / 10]), \end{aligned} \tag{5}$$

where $T_1 = 20$ °C, $T_2 = 300$ °C and $T_3 = 700$ °C, W is the water flux in l/(m^2 s).

The thermophysical coefficients were calculated at each position and they depend on the transformed fraction and temperature as described by the following equation:

$$\begin{aligned} c &= \chi_\gamma c_\gamma + (\chi_f + \chi_b + \chi_m) c_\alpha, \\ \kappa &= \chi_\gamma \kappa_\gamma + (\chi_f + \chi_b + \chi_m) \kappa_\alpha, \\ \rho &= \left(\frac{\chi_\gamma}{\rho_\gamma} + \frac{(\chi_f + \chi_b + \chi_m)}{\rho_\alpha} \right)^{-1} . \end{aligned} \tag{6}$$

The latent heat L released to austenite decomposition during a time step Δt is included in the simulations using the following equation:

$$s = \rho_\gamma L \frac{\partial}{\partial t} (\chi_f + \chi_b + \chi_m), \tag{7}$$

where L is calculated as in [10].

2.2.1. 1-dimensional heat conduction

A one dimensional simulation code was created to enable the optimization of cooling procedures by testing the outcome of varying different parameters. The advantage of this model is the short calculation time, while still

providing reasonable accuracy and fundamental physical basis. A finite element (FE) method for solving of the heat equation (3) was implemented by discretizing the spatial coordinate with the Galerkin method and the time coordinate with explicit Euler method [13].

2.2.2. 2-dimensional heat conduction

In order to examine in more detail the heat conduction and transfer, we implemented an explicit 2-dimensional finite difference (FD) method for solving the heat equation (3). Due to relative simplicity of the method, it can be shortly described here in detail. Taking in to account the spatial dependence of the heat conductivity, κ, the equation (3) can be written as follows:

$$\rho c \frac{\partial}{\partial t} T = \nabla \kappa \bullet \nabla T + \kappa \nabla^2 T + s = \frac{\partial \kappa}{\partial x_1}\frac{\partial T}{\partial x_1} + \frac{\partial \kappa}{\partial x_2}\frac{\partial T}{\partial x_2} + \kappa\left(\frac{\partial^2 T}{\partial x_1^2} + \frac{\partial^2 T}{\partial x_2^2}\right) + s \ . \tag{8}$$

The derivatives can then be replaced by the difference approximations

$$\begin{aligned}
\frac{\partial \kappa}{\partial x_i} &= \frac{1}{2}\left(\frac{\kappa(x_i + \Delta x_i, t) - \kappa(x_i, t)}{\Delta x_i} + \frac{\kappa(x_i, t) - \kappa(x_i - \Delta x_i, t)}{\Delta x_i}\right), \\
\frac{\partial T}{\partial x_i} &= \frac{1}{2}\left(\frac{T(x_i + \Delta x_i, t) - T(x_i, t)}{\Delta x_i} + \frac{T(x_i, t) - T(x_i - \Delta x_i, t)}{\Delta x_i}\right), \\
\frac{\partial^2 T}{\partial x_i^2} &= \frac{1}{\Delta x_i}\left(\frac{T(x_i + \Delta x_i, t) - T(x_i, t)}{\Delta x_i} - \frac{T(x_i, t) - T(x_i - \Delta x_i, t)}{\Delta x_i}\right), \\
\frac{\partial T}{\partial t} &= \frac{T(x, t + \Delta t) - T(x, t)}{\Delta t},
\end{aligned} \tag{9}$$

where the index i is used to denote the two coordinates x_1 and x_2. Once the derivatives in Eq. (8) are replaced by the respective difference approximations described by Eq. (9), the temperature on the next time step, $T(x, t+\Delta t)$ is solved. On the points located at the surfaces, the discrete spatial derivative $[T(x_i,t)\text{-}T(x_i\text{-}\Delta x_i,t)]/\Delta x_i$ and $[T(x_{i+}\Delta x_i,t)\text{-}T(x_i,t)]/\Delta x_i$ are replaced by the gradient obtained from Eq. (4). The FD code was parallelized with OpenMP library.

3. Materials and methods

Dilatation data for the CCT diagrams simulated with and without prior strain using a Gleeble 3800 simulator, samples from steel (base: 0.1C-0.2Si-1.1Mn-0.15Mo-0.03Ti-0.002B in wt.%) were initially solution treated at 1250 °C for 2 hours followed by water quenching. Cylindrical specimens of 6 mm dia x 9 mm for linear cooling rates 2–40 °C/s and 4 mm dia x 6 mm for cooling rates 50 °C/s, 60°C/s and 70 °C/s were used for the CCT dilatation tests. Before compressing, samples were heated at 10 °C/s to 1100 °C, held for 2 min, cooled to 850 °C, held 15 s, and then compressed with three hits each having a strain of ~0.2 at a strain rate of 1/s. The specimens were then held 5 s before cooling at various linear rates in the range 2–70 °C/s. Similarly, the undeformed specimens were reheated in a similar manner, held for 2 min prior to cooling at different linear cooling rates 2–70 °C/s. Different phase transformation temperatures were identified from the temperature-dilatation data based on the deviation from the linear thermal contraction. Furthermore, a general characterization of the transformation microstructures was performed with a field emission scanning electron microscope (FESEM) (Ultra plus, Zeiss) on specimens etched with nital. More specific information of the material phase transformation and microstructures is presented in Ref. [14].

4. Results and discussion

The model parameters were numerically fitted by minimizing the difference between the computed and experimentally determined temperatures, where 12.5, 25, 50, 75 and 87.5 % austenite was transformed. We programmed a Matlab script which passed arguments to our phase transformation software and read back the results after calculation. Matlab fminsearch function, which uses the Nelder-Mead algorithm [15], was applied for the minimization. The fitted model parameters for ferrite and bainite are shown in Table 1. For martensite transformation, the parameters $\eta = 0.1164$ and $M_s = 491.0$ °C were obtained.

Table 1. Fitted model parameters for ferrite and bainite transformation.

Product	K	A (°C)	m	Q (kJ)	a	b	c	n
Ferrite	7.952×10^{7}	736.6	8.937	196.7	2.666×10^{-3}	573.8	5.879	2.423
Bainite (T > 527.0 °C)	4.513	623.5	1.536	37.9	3.780×10^{-3}	527.0	1.183	0.992
Bainite (T ≤ 527.0 °C)	4.513	623.5	1.536	37.9	1.825×10^{-5}	527.0	1.183	0.992

We used the actual measured cooling paths for the fitting calculations, since, although the physical thermomechanical Gleeble simulator is programmed to maintain constant cooling rates, the rapid release of latent heat caused deviation from the linear cooling paths, as shown in Fig. 1(a). The comparison of the experimentally determined fraction transformed to the calculated values after the fitting is shown in Fig. 1(b). We also checked that calculated values were in reasonable agreement with the estimated final fractions of ferrite, bainite and martensite obtained from microscopy after cooling

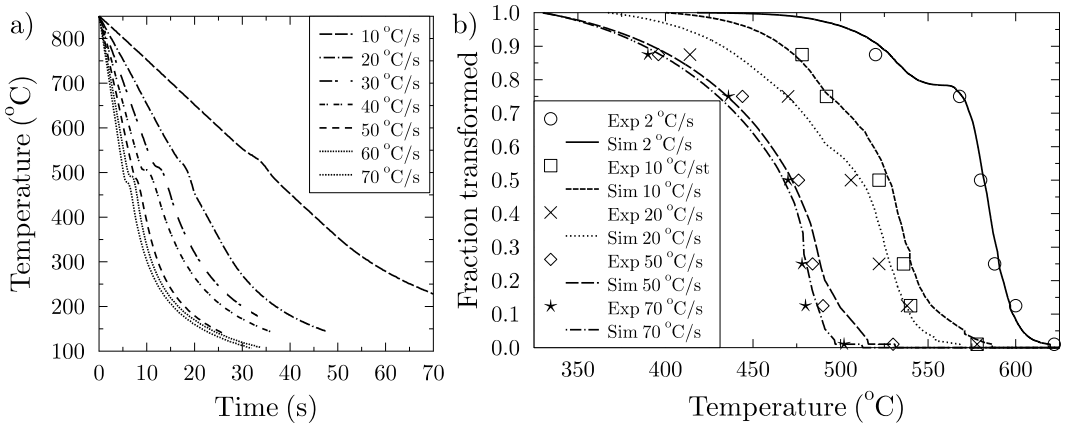

Fig. 1. (a) Experimental cooling paths used in fitting of model show deviation from linear cooling path due to latent heat released during transformation; (b) Comparison of fitted model to the experimental values of transformed fraction at different temperatures during cooling.

To exemplify the developed simulation methods, we applied them in the following test cases which resemble realistic cooling procedures. We emphasize that the heat transfer parameters and water impingement areas need to be calibrated against experimental data in order to obtain accurate results in realistic setting. Using our 1-dimensional heat conduction code, we simulated a steel strip moving with 3.1 m/s speed. Above and below of the strip 36 mm width water spray cooling zones were assumed located periodically every 0.6 m. Water flux of 707 l/(m^2 s) was assumed on the spray zones above of the strip and twice this amount for the spray zones below of the strip. Above of the strip we additionally assumed effective heat transfer coefficien h_{eff} = 500 for the areas which were not under the spray zone, to mimic water film boiling.

The temperature distribution at the bottom surface, quarter thickness (below the midpoint) and in the middle of the strip is shown in Fig. 2.(a)) The result shows that while the surface undergoes deep oscillations in temperature, the quarter and middle parts of the strip are cooled in relatively stable rates. The midpoint curve shows temperature rise due to latent heat released from bainitic and martensitic transformations. The bainite and martensite formed at quarter depth and in the middle of the strip are plotted as function of time in Fig. 2(b)). The bottom surface was transformed fully in to martensite during cooling.

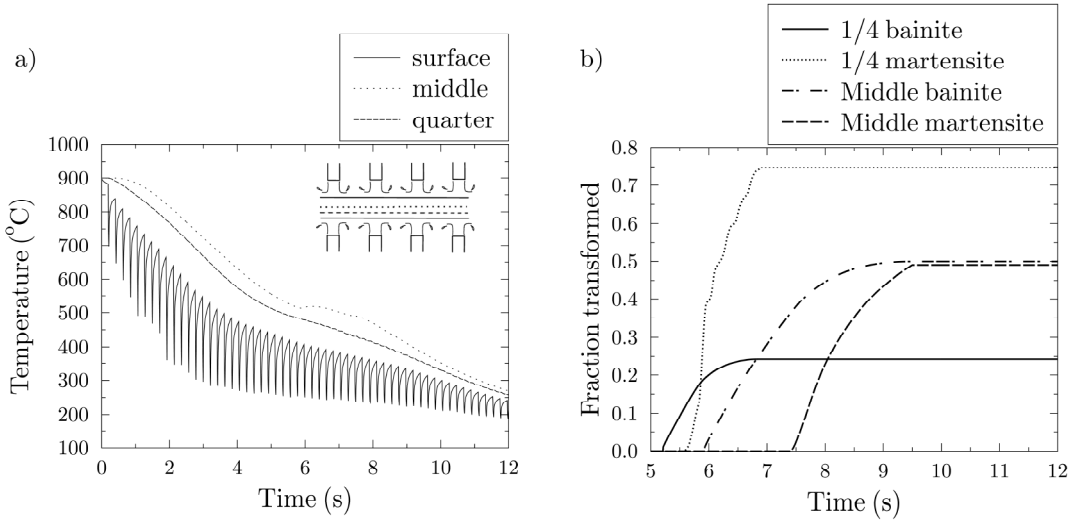

Fig. 2. (a) Simulated temperature on surface, in middle and at quarter thickness of moving strip obtained using our 1-dimensional FE code during cooling with repeated array of cooling sprays illustrated in inset (b) fractions of bainite and martensite formed at surface and in middle of strip as function of time.

The 2-dimensional heat conduction and transfer simulations were used to obtain the temperature disribution while the material was simulated moving under the spray water cooling zone. The temperature is plotted near the surface, quarter thickness and in the middle of the strip as function of position along the strip in Fig. 3.

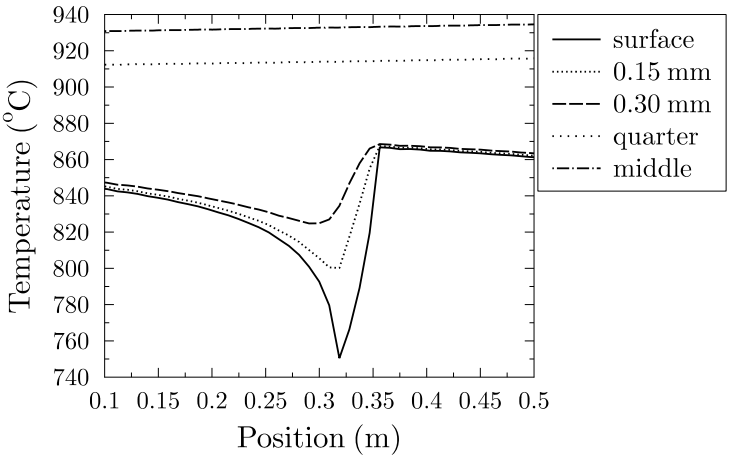

Fig. 3. Temperature as function of position along strip on surface and subsurface region, at quarter thickness and in middle of strip obtained from our 2-dimensional FD model during water shower moving to positive direction of x-axis relative to strip (i.e. the strip is moving to the left).

The focus of the current article is in providing computational framework for simulating phase transformation behaviour of steel strip in fully coupled manner with heat transfer and conduction. In future work we will focus on calibrating the heat transfer coefficient of the current model using experimentally measured thermal histories during water spray cooling in realistic strip cooling conditions.

Acknowledgements

We would like to thank the staff of the Materials and Production Technology laboratory in the University of Oulu for their work in conducting the experiments.

References

[1] J. Ilmola, A. Pohjonen, O. Seppälä, O. Leinonen, J. Larkiola, J. Jokisaari, E. Putaansuu, P. Lehtikangas, Coupled multiscale and multiphysical analysis of a hot steel strip mill and microstructure formation during water cooling, Submitted for publication in Metal Forming 2018 conference proceedings.

[2] J. Kirkaldy, R. Sharma, A new phenomenology for IT and CCT curves, Scripta Metallurgica, 16 (1982) 1193–1198.

[3] T. Pham, E. Hawbolt, J. Brimacombe, Predicting the onset of transformation under noncontiunuous cooling conditions 1. theory, Metallurgical and Materials Transactions A, 26 (1995) 1987–1992.

[4] A. Pohjonen, A. Kaijalainen, M. Somani, J. Larkiola, Analysis of bainite onset during cooling following prior deformation at different temperatures, Computer Methods in Materials Science, 17 (2017) 30–35.

[5] J. Leblond, G. Mottet, J. Devaux, J.C. Devaux, Mathematical models of anisothermal phase transformations in steels, and predicted plastic behaviour, Matrials Science and Technology, 1 (1985) 815–822.

[6] A. Pohjonen, J. Paananen, J. Mourujärvi, T. Manninen, J. Larkiola, D. Porter, Computer simulations of austenite decomposition of microalloyed 700 MPa steel during cooling, Accepted for publication in Esaform 2018 conference proceedings.

[7] B. Donnay, J.C. Herman, V. Leroy, U. Lotter, R. Grossterlinden, H. Pircher, Microstrucrure evolution of C-Mn steels in the hot deformation process: the stripcam model, 2nd International Conference on Modeling of Metal Rolling Processes, Eds. J.H. Beynon, P. Ingham, H. Teichert, K. Waterson, (1996) 113–122.

[8] D.C. Martin, Selected heat conduction problems in thermomechanical treatment of steel, Juvenes Print, Tampere, (2011).

[9] D. Koistinen, R. Marburger, A general equation prescribing the extent of the austenite-martensite transformation in pure iron-carbon alloys and plain carbon steels, Acta Metallurgica, 7 (1959) 59–60.

[10] K.M. Browne, Modelling the thermophysical properties of iron and steels, Proceedings of Materials 98 – The Biennial Conference of the Institute of Materials Engineering, Ed. Michael Ferry, (1983) 433–438.

[11] J. Miettinen, Calculation of solidification related thermophysical properties for steels, Metallurgical and Materials Transactions B, 28B (1997) 281–297.

[12] P.D. Hodgson, K.M. Browne, D.C. Collinson, T.T. Pham, R.K. Gibbs, A mathematical model to simulate the thermomechanical processing of steel, Quenching and Carburising, Internationa federation for heat treatment and surface engineering, Melbourne, (1991) 139–159.

[13] J. Hämäläinen, J. Järvinen, Elementtimenetelmä virtauslaskennassa, CSC – Tieteellinen laskenta Oy, ISBN 952-5520-20-X, (2006).

[14] A. Kaijalainen, N. Vähäkuopus, M. Somani, S. Mehtonen, D. Porter, J. Kömi, The effects of finish rolling temperature and niobium microalloying on the microstructure and properties of a direct quenched high-strength steel, Archives of Metallurgy and Materials, 62 (2017) 619–626.

[15] Matlab documentation, https://se.mathworks.com/help/, retrieved 28.2.2018.